electronics

MDPI

Article

A Multi-Zone Temperature Control Model in an IoT Environment for the Cold Chain Using the Elephant Herding Optimization Algorithm

Oskar Skubisz [1], Hubert Zarzycki [2,*], Marta Wincewicz Bosy [1], Małgorzata Dymyt [1] and Piotr Kardasz [3,4]

[1] Logistics Department, General Tadeusz Kościuszko Military University of Land Forces, 51-147 Wroclaw, Poland; oskar.skubisz@awl.edu.pl (O.S.)
[2] Faculty of Computer Science and Technology, Wroclaw University of Science and Technology, 50-370 Wroclaw, Poland
[3] Institute of Computer Science, University College of Professional Education, 53-329 Wroclaw, Poland
[4] Automation and Robotics Department, Technical Academy of Informatics in Applied Sciences, 54-239 Wroclaw, Poland
* Correspondence: hubert.zarzycki@pwr.edu.pl

Abstract

The article presents the development of a multi-zone temperature control model in an Internet of Things (IoT) environment, designed for the cold chain of pharmaceutical products transported by sea. The model is based on the Elephant Herding Optimization (EHO) algorithm, which is used to regulate cooling modes in three independent temperature zones. The study is designed as a simulation-based proof-of-concept rather than as a full-scale experimental validation on an industrial refrigerated container. The proposed framework evaluates whether an EHO-based controller can generate spatially differentiated cooling decisions under synthetic but controlled disturbance scenarios. The variability of sensor readings reflects conditions typical of long-distance maritime transport. These include transitions across different climate zones, changes in solar exposure, and local differences in thermal load. The simulation results indicate that EHO maintains the temperature within the target range required for pharmaceutical cargo, i.e., 0–8 °C. The algorithm responds effectively to local disturbances and to asymmetry between zones. The proposed model provides a basis for further research on autonomous monitoring and control methods in IoT-based cold chain systems; however, validation using measurements from real refrigerated containers, physical heat-transfer modelling, refrigeration-unit response delays, and IoT communication disturbances remains necessary before operational deployment.

Keywords: cold chain; Internet of Things (IoT); temperature control; multi-zone control model; pharmaceutical transport; maritime logistics; nature-inspired metaheuristics; Elephant Herding Optimization (EHO); real-time monitoring systems; simulation modelling

Check for updates

Academic Editor: Jin Huang

Received: 27 April 2026
Revised: 3 June 2026
Accepted: 10 June 2026
Published: 18 June 2026

Copyright: © 2026 by the authors. Licensee MDPI, Basel, Switzerland. This article is an open access article distributed under the terms and conditions of the Creative Commons Attribution (CC BY) license.

1. Introduction

Maintaining stable environmental parameters in the cold chain is a condition for preserving the quality integrity of sensitive cargo. This includes both finished medicinal products and active pharmaceutical ingredients (APIs) transported between seaports, temporarily stored in terminal infrastructure, and handled during transshipment operations. The complexity of modern, multi-node logistics networks means that temperature, humidity, and exposure time must be monitored continuously at the levels of transport, storage,

and port handling. This gives the analysed problem a clear systemic and technological dimension within global goods flows [1].

With the increasing complexity of global transport networks, especially in maritime logistics, the need for continuous supervision of environmental parameters becomes not only a technically demanding task but also an important managerial problem. The simultaneous observation, analysis, and interpretation of data generated by IoT infrastructure reveal the scale of challenges associated with temperature fluctuations between zones, their operational causes, and their consequences for the integrity of sensitive cargo [2].

The Internet of Things architecture used in monitoring and control systems is characterised by a high degree of distribution and by functional diversity across its individual layers. These layers include sensor networks, data processing methods, and the use of cloud-based technologies and resources. Such solutions operate in environments where network load, the dynamics of information flows, and environmental conditions change continuously over time [3]. For this reason, maintaining measurement stability and continuity of data transmission becomes one of the main design challenges, especially in applications that require supervision of parameters directly related to product quality.

In the cold chain of pharmaceutical products, the role of IoT solutions extends beyond the mere recording of temperature. Sensors placed in different parts of the cargo space reveal the heterogeneity of thermal conditions. This heterogeneity results from differences in insulation, thermal load, and exposure to external factors characteristic of maritime transport. As a result, maintaining stable environmental parameters is no longer only a matter of controlling a single measurement point. It becomes a regulation problem in a multi-zone system, in which each zone responds differently to the same ambient conditions. This complexity means that traditional control methods, based on simple thresholds or deterministic relationships, have a limited ability to adapt to dynamic temperature changes observed in operational practice. For this reason, the literature increasingly proposes approaches based on nature-inspired algorithms. Such methods are capable of operating under incomplete information, local disturbances, and variable data streams derived from the analysis of the surrounding environment [4].

Metaheuristics of this type not only represent relationships between multiple components of a system but also enable control decisions to be adjusted in real time on the basis of changing measurement data. In the pharmaceutical cold chain, where the acceptable temperature range is narrow and deviations have a direct impact on cargo quality, the need for such solutions is particularly evident. However, despite the growing number of studies on IoT in logistics, there remains a clear research gap in the area of multi-zone temperature control that simultaneously accounts for the operational characteristics of maritime transport. Existing studies only to a limited extent address the problem of spatially differentiated thermal conditions in refrigerated containers, where each zone may require a separate regulatory response. This gap concerns both the algorithmic layer, related to the selection and adaptation of the control mechanism, and the operational layer, related to the practical interpretation of sensor data in a dynamic transport environment. Filling this gap requires an approach that combines simulation modelling with adaptive decision-making methods. In response to this need, this article proposes a multi-zone temperature control model based on IoT infrastructure and the Elephant Herding Optimization algorithm. The model enables dynamic regulation of environmental parameters in the cold chain of pharmaceutical products. The importance of such solutions becomes particularly visible in the context of developing smart port concepts, where the integration of intelligent sensors, wireless networks, and analytical systems provides a basis for advanced container monitoring and improved safety of transport conditions [5].

Recent maritime-logistics studies also show that data-driven and optimization-based approaches are increasingly used to support complex port and shipping operations. Yu et al. proposed a method combining graph theory and time-series analysis for fine-grained traffic-flow prediction in port areas, demonstrating the relevance of spatio-temporal modelling for maritime decision support [6]. In another study, Yu et al. developed an optimization-based framework for global LNG shipping-network management aimed at reducing emissions, showing the importance of optimization methods in large-scale maritime transport systems [7]. Although these studies address different operational problems, they confirm the growing role of analytical and optimization-based methods in maritime logistics. The present work extends this general direction to the more specific problem of adaptive temperature control in the pharmaceutical cold chain.

The main contributions of this study are as follows. First, the article formulates a simulation-based multi-zone control problem for pharmaceutical cold-chain transport in a maritime logistics context, where thermal conditions differ between container zones. Second, it adapts the Elephant Herding Optimization algorithm to a discrete control space consisting of three cooling modes: Low, Medium, and High. Third, it introduces control maps as an interpretive tool for analysing not only temperature trajectories but also the spatial and temporal structure of cooling-mode decisions. Fourth, it provides a quantitative self-made simulation framework for assessing temperature-limit violations, cooling-mode switching, and the distribution of control actions across zones. These contributions should be interpreted as a proof-of-concept for adaptive IoT-based cold-chain control, not as a replacement for physical validation on a real refrigerated container.

2. Nature-Inspired Algorithms

The use of computational methods in IoT environments, especially in systems that require continuous responses to changing operational conditions, leads to the adoption of approaches capable of functioning under incomplete information, local disturbances, and dynamic data structures. Over the last two decades, methods inspired by processes observed in nature have played a particularly important role in this area. These algorithms refer to biological, social, and physical phenomena, treating them as models for solution search. They are applied wherever deterministic approaches fail because of system complexity, variability, or the absence of precise analytical relationships [8].

Metaheuristics now form a broad class of optimization methods developed at the intersection of computer science, applied mathematics, and the natural sciences. They share the use of processes observed in nature, including population dynamics, collective animal behaviour, and physical phenomena, as heuristic models for searching complex decision spaces [9–12]. Nature-inspired algorithms are therefore suited to large, heterogeneous, and dynamic solution spaces, where conventional optimization techniques face computational limitations [13–17].

In the metaheuristic approach, the aim is not to reproduce biological phenomena literally, but to use their structural properties, especially adaptation mechanisms, to build procedures for the iterative improvement of solutions in complex decision spaces. These algorithms combine randomness, diversification, and gradual intensification of the search. This enables them to address problems that lack clear analytical models. For this reason, metaheuristics have become widely used in tasks requiring the exploration of multidimensional and dynamic decision spaces. Their interdisciplinary design also supports adaptation to a broad range of applications, from robotics and data analysis to logistics and cyber–physical systems [18–26].

Contemporary metaheuristics are among the main computational approaches used in systems operating under variable and partly uncertain environmental conditions. Their

design allows exploration and adaptive exploitation of decision spaces to be balanced, supporting both global and local search. This property is particularly relevant in IoT environments, where data arrive as streams and control parameters must be updated continuously. In logistics, especially in the cold chain, metaheuristics provide a framework for formulating control decisions when complete physical models are unavailable or when existing models do not allow precise analysis of multi-zone systems. Population-based algorithms are especially relevant in this context, as they can represent the dynamics of distributed systems and adapt the behaviour of individual solutions to local disturbances and changing operating conditions. One such algorithm is Elephant Herding Optimization, whose properties make it a justified candidate for controlling environmental parameters in IoT infrastructure [27,28].

Optimization and Control Methods in Cold-Chain Temperature Regulation

Temperature regulation in cold-chain systems can be approached using several classes of methods. The simplest group includes threshold-based controllers, in which the cooling mode is changed when the measured temperature exceeds predefined limits. Such methods are easy to implement and computationally inexpensive, but they may generate frequent switching and do not explicitly account for spatial heterogeneity inside a container. PID controllers are widely used in industrial regulation tasks and can provide smooth control when a reliable dynamic model or well-tuned feedback loop is available. However, tuning becomes more difficult when the object is spatially heterogeneous and when each zone responds differently to external disturbances.

Model predictive control (MPC) is a more advanced approach because it can optimize future control actions under constraints. In the context of refrigerated containers, MPC would require a sufficiently accurate thermal model, including heat transfer, airflow, cargo load, actuator dynamics, and response delays. This is a strong advantage when such a model is available, but it also increases modelling effort and computational requirements. Population-based metaheuristics, including genetic algorithms (GA), particle swarm optimization (PSO), ant colony optimization (ACO), and EHO, provide an alternative when the decision space is discrete, nonlinear, or only partly described by analytical relationships [29–34].

In this study, EHO was selected because it combines local exploitation within clans with global exploration through the migration mechanism. This structure is suitable for a multi-zone control problem in which individual zones may require different corrective actions. The purpose of using EHO is not to claim general superiority over PID, MPC, PSO, GA, or ACO, but to test whether its population-based search mechanism can produce spatially differentiated cooling decisions in a discrete IoT-based simulation environment. A systematic comparison (Table 1) with these methods is therefore identified as a necessary direction for further work.

Table 1. Qualitative comparison of selected control and optimization methods for cold-chain temperature regulation.

Method	Main Advantage	Main Limitation in the Present Problem
Threshold-based control	Simple, fast, easy to implement	May cause frequent switching and does not optimize multi-zone decisions
PID	Smooth feedback control for well-tuned systems	Requires careful tuning and is less direct for discrete multi-zone decisions
MPC	Handles constraints and prediction horizon	Requires a reliable physical model and higher computational effort

Table 1. *Cont.*

Method	Main Advantage	Main Limitation in the Present Problem
GA	Flexible search in discrete spaces	May require many evaluations and parameter tuning
PSO	Efficient population-based search	Originally continuous; discrete adaptation is required
ACO	Useful for combinatorial decisions	Less direct for continuous thermal-state feedback
EHO	Combines clan-based exploitation and migration-based exploration	Requires discretization, parameter setting, and benchmark validation

3. Application of the Modified Elephant Herding Algorithm in an IoT Environment for the Cold Chain

3.1. Fundamentals of the Elephant Herding Optimization (EHO) Algorithm

The Elephant Herding Optimization (EHO) algorithm, proposed by Wang, Deb, and Coelho, belongs to the group of population-based optimization methods inspired by the social structures of elephants [21]. In natural conditions, elephant herds form stable matriarchal clans, in which movement dynamics are guided by an experienced female. Individuals within a clan tend to gather around the leader, whereas adult males leave the herd and move independently, exploring new areas of the environment. This concept was translated into two coexisting computational mechanisms: local search performed within clans and global exploration carried out by males.

In the simulation configuration used in this study, the EHO population consisted of three clans, with five individuals in each clan. Thus, the total population size was 15 candidate solutions. Each individual encoded three decision variables corresponding to the cooling modes in the three container zones. The maximum number of internal optimization iterations at each decision step was set to 50. The movement coefficient was implemented as a bounded random perturbation in the interval $[-0.1, 0.1]$ for each decision dimension. The stopping criterion was therefore the completion of the predefined number of iterations. These values were selected to keep the computational burden low while maintaining a sufficient number of candidate solutions for a three-dimensional discrete control problem.

In the classical version of EHO, the population is divided into K clans. In each clan, a leader is identified as the best individual. The position of each elephant within the clan is updated by moving it towards the local optimum represented by the matriarch:

$$X_i^{t+1} = X_m^t + \alpha * \left(X_m^t - X_i^t\right) \quad (1)$$

where X_m^t denotes the position of the matriarch, X_i^t denotes the position of an individual, and α is a coefficient defining the intensity of movement towards the leader. This mechanism is responsible for exploitation, understood as the refinement of promising regions of the solution space. It is complemented by the male migration rule, which generates new points in the space of feasible solutions according to the following model:

$$X_i^{t+1} = X_{min} + r * \left(X_{max} - X_{min}\right) \quad (2)$$

where r is a random variable, while X_{min} and X_{max} define the boundaries of the search space. This mechanism performs an exploratory function, enabling the algorithm to move beyond local extrema.

The operation of the classical EHO can be presented in the following simplified scheme:
Pseudocode—classical version of EHO

1. Initialization of the population and division into clans.
2. Evaluation of the quality of all individuals.
3. For each clan:
   - Identification of the matriarch;
   - Update of the positions of females and young males;
   - Migration of adult males.
4. Elitist preservation of the best solution.
5. Continuation of iterations until the stopping condition is met.

The EHO mechanism combines intensification and exploration, which enables it to search decision spaces with a large number of dimensions and a discontinuous structure. In this study, the classical version of the algorithm serves as the starting point for developing a variant adapted to multi-zone temperature control in an IoT environment.

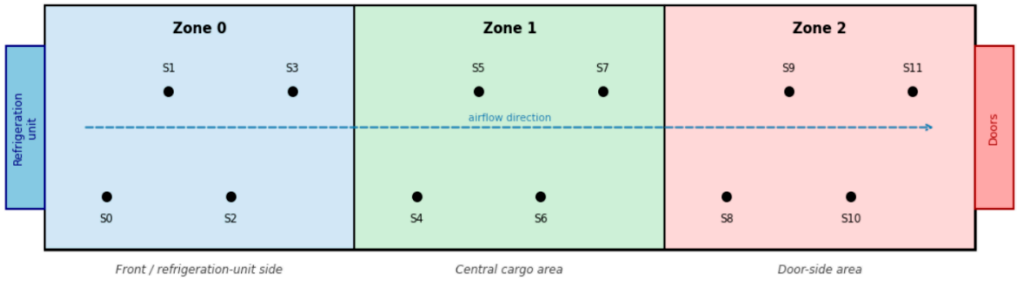
3.2. Multi-Zone Temperature Control Model in IoT Infrastructure

The study used synthetic temperature data generated on the basis of a model assuming nonlinear and asynchronous temperature changes in each zone. These data reflect typical operating conditions encountered during maritime transport, including transitions across different climate zones, the impact of solar radiation, and differences in insulation between zones. The synthetic sequences include both slow upward or downward temperature trends and sudden low-amplitude jumps. These represent random disturbances observed in real IoT systems. The use of synthetic data made it possible to fully control the range and character of environmental disturbances. It also enabled the algorithm to be evaluated across a broad spectrum of scenarios, without limitations resulting from the availability of measurement data.

The model developed in this study reflects the conditions inside a refrigerated container used in the cold chain of pharmaceutical products. The cargo space was divided into three independent temperature zones. Each zone responds differently to environmental changes resulting from differences in insulation, local heat sources, solar radiation, and external conditions typical of maritime transport. A network of virtual IoT sensors was placed in each zone. These sensors continuously transmit temperature data, which provide the basis for control decisions.

The three-zone structure was defined as an abstract spatial partition of the container cargo space. Zone 0 represents the front part of the container, located closer to the refrigeration unit. Zone 1 represents the central cargo area, and Zone 2 represents the door-side area, which is typically more exposed to thermal disturbances caused by weaker insulation and door operations. This partition is a simplified representation used for simulation purposes; it does not reproduce the full airflow structure of a specific commercial refrigerated container.

The spatial layout of the three zones and the sensor distribution are illustrated in Scheme 1 below. Four virtual temperature sensors were assigned to each zone (S0–S3 in Zone 0, S4–S7 in Zone 1, and S8–S11 in Zone 2), giving twelve sensors in total. The zone-level temperature used by the controller was calculated as the arithmetic mean of the readings from the four sensors in each zone, as defined in Equation (X).



Scheme 1. Schematic representation of the three-zone temperature-control model and virtual sensor layout used in the simulation.

Zone 0 is located closest to the refrigeration unit (front), Zone 1 represents the central cargo area, and Zone 2 is located on the door side. Four virtual temperature sensors (S0–S3, S4–S7, S8–S11) are assigned to each zone. The dashed arrow indicates the assumed direction of cold airflow. The spatial partition is a simplified simulation construct and does not represent the airflow geometry of a specific commercial refrigerated container.

Twelve virtual temperature sensors were assigned to the container, with four sensors per zone. The zone-level temperature used by the controller was calculated as the arithmetic mean of the readings from sensors assigned to a given zone:

$$T_i(t) = \frac{1}{n_i}\sum_{j\in\mathcal{S}i} T_{ij}(t),\ i = 1,2,3 \tag{3}$$

where $T_{ij}(t)$ is the reading of sensor j assigned to zone i, $\mathcal{S}_i$ is the set of sensors in zone i, and $n_i = |\mathcal{S}_i|$ is the number of sensors in that zone. In the present simulation, $n_i = 4$ for each zone. This aggregation method was selected because the aim of the study was to analyse zone-level control decisions rather than local sensor-level heat-transfer phenomena.

In the adopted approach, the cooling system is assumed to offer a set of discrete operating modes corresponding to different levels of heat exchange intensity. These modes can be changed independently for each zone, allowing flexible control under conditions of spatial temperature asymmetry. Sensor readings are updated at time steps Δt, which represent successive decision points of the algorithm. At each step, the system must determine the cooling intensity for each zone in order to maintain the temperature within the 0–8 °C range, while avoiding an excessive number of abrupt changes in operating mode.

Temperature variability in the model results from two main categories of factors: environmental influences and local disturbances. Changes in ambient temperature, associated with the container passing through different climate zones, affect the cooling system through the container's insulating shell. This leads to gradual heating or cooling of individual zones. The dynamics of these processes are nonlinear and difficult to represent unambiguously in a classical analytical model. These phenomena are consistent with the behaviour of real monitoring systems and reflect the operational limitations faced by cold chain operators in maritime logistics.

The resulting multi-zone control architecture requires an approach capable of operating under variable, partly uncertain conditions and under delayed thermal responses. This provides a natural justification for the use of metaheuristics, including the proposed variant of the EHO algorithm.

Synthetic Temperature-Data Generation Model

The simulation used synthetic temperature sequences in order to test the control algorithm under reproducible and controllable disturbance conditions. The generated data were not calibrated using measurements from a specific refrigerated container. Instead, they

were designed to reproduce general qualitative features of maritime cold-chain transport: gradual thermal drift, asynchronous zone behaviour, and occasional local disturbances.

For each zone, the temperature state was updated at discrete time steps according to the following simplified model:

$$T_i(t + \Delta t) = \text{clip}_{[0,8]}(T_i(t) + d_i(t) - c(x_i(t)) + \varepsilon_i(t) + q_i(t)) \tag{4}$$

here $T_i(t)$ is the temperature in zone (i), ($d_i(t)$) represents slow environmental drift, $c(x_i(t))$ is the cooling effect associated with the selected cooling mode, $\varepsilon_i(t)$ is a random low-amplitude disturbance, and $q_i(t)$ is an occasional impulse disturbance. The operator $\text{clip}_{[0,8]}(\cdot)$ tricts simulated values to the admissible pharmaceutical cold-chain range used in this study.

The stochastic component was implemented as follows:

$$\varepsilon_i(t) \sim U(-0.5, 0.5) \tag{5}$$

and, with probability $p_q = 0.05$, an additional impulse disturbance was generated:

$$q_i(t) \sim U(-1.5, 1.5) \tag{6}$$

The cooling mode was represented by three discrete levels:

$$c(x_i) = \begin{cases} c_L, & x_i = 0 \ \ Low, \\ c_M, & x_i = 1 \ \ Medium, \\ c_H, & x_i = 2 \ \ High, \end{cases} \qquad c_L < c_M < c_H \tag{7}$$

In the simplified implementation used for the reported simulation, the control logic selected High mode when the zone temperature exceeded 6 °C, Medium mode when the temperature was between 3 °C and 6 °C, and Low mode otherwise. This threshold mapping was used as the operational discretization layer for generating interpretable cooling-mode sequences. The EHO mechanism was used to search candidate control settings and to represent local adaptive decision-making in the three-zone space. This simplification is now explicitly stated because the model does not yet include a full physical heat-transfer equation or actuator-delay dynamics.

3.3. Solution Representation and Structure of the Search Space

In the proposed control model, each individual in the EHO population represents a set of regulatory decisions concerning the cooling intensity in the three container zones. This division reflects the actual thermal structure of refrigerated containers, where a persistent temperature gradient can be observed. The lowest values usually occur in the front section, located near the refrigeration unit. The middle zone is characterised by the greatest stability, whereas the largest temperature deviations are recorded near the doors, which constitute the weakest insulation point. Including this heterogeneity in the model structure allows operating conditions to be represented more accurately and enables a more precise assessment of the control algorithm. The representation was adopted in the form of a discrete vector:

$$x = [x_1, x_2, \ x_3] \tag{8}$$

where each component describes the cooling mode in the corresponding zone. The set of admissible values is defined as follows:

$$x_i \in \{0, 1, 2\}, \quad i = 1, 2, 3. \tag{9}$$

where 0 = Low, 1 = Medium, 2 = High.

This structure enables the direct representation of the system's spatial heterogeneity. It also ensures consistency with real control mechanisms used in refrigerated containers during maritime transport, temporary terminal storage, and transshipment operations.

3.4. Objective Function for Temperature Control in a Cold Chain Container

The objective of the control process is to maintain the temperature in each container zone within the required range of 0–8 °C, while limiting an excessive number of cooling mode switches. The objective function must therefore account for both deviation from the target temperature and the stability of regulatory actions. This is justified by the specific requirements of pharmaceutical transport. Excessively frequent changes in cooling intensity may lead to system instability, increased energy consumption, and greater exposure to thermal risk.

At each decision step, the controller receives the vector of current zone temperatures:

$$T(t) = [T_1(t), T_2(t), T_3(t)] \tag{10}$$

For each candidate control vector, the algorithm estimates a one-step-ahead temperature response:

$$\hat{T}_i(t + \Delta t \mid x_i(t)) = T_i(t) + \hat{di}(t) - \gamma x_i + \hat{\varepsilon}_i(t) \tag{11}$$

where $\hat{di}(t)$ denotes the estimated local thermal drift, γx_i denotes the cooling effect assigned to the selected mode x_i, and $\hat{\varepsilon}_i(t)$ represents the expected local disturbance term. The cooling effect satisfies $\gamma_0 < \gamma_1 < \gamma_2$, corresponding to Low, Medium, and High cooling intensity, respectively. This one-step response model allows different candidate control vectors to produce different predicted temperatures and therefore prevents the objective function from degenerating into a switching-only criterion.

The corresponding vector of control decisions is defined as:

$$x(t) = [x_1(t), x_2(t), x_3(t)],\ x_i(t) \in 0, 1, 2 \tag{12}$$

The value of the objective function was then defined as the sum of a predicted temperature-limit violation component and a switching penalty:

$$F(x(t)) = w_1 E(t + \Delta t \mid x(t)) + w_2 S(t) \tag{13}$$

The predicted temperature component is calculated as:

$$E(t + \Delta t \mid x(t)) = \sum_{i=1}^{3} \left[\max\left(0, \hat{T}_i(t + \Delta t \mid x_i(t)) - 8\right) + \max\left(0, -\hat{T}_i(t + \Delta t \mid x_i(t))\right)\right] \tag{14}$$

Thus, a candidate solution is penalized only if its predicted next-step temperature violates the admissible interval. This formulation explicitly links the decision vector (x(t)) with the expected thermal state at $t + \Delta t$.

(1) Temperature component

The temperature deviation from the admissible range is formalized as:

$$E(t) = \sum_{i=1}^{3} \left(max(0, T_i(t) - 8) + \max(0,\ -T_i(t))\right) \tag{15}$$

where $T_i(t)$ denotes the temperature in zone i at time t. The component $E(t)$ takes a positive value only when the temperature exceeds the admissible range of 0–8 °C. Values within this interval are not penalized, which allows the algorithm to focus on actual thermal deviations rather than on natural fluctuations inside the acceptable range.

(2) Stabilizing component

The second part of the objective function limits the abruptness of changes in cooling modes:

$$S(t) = \sum_{i=1}^{3} |x_i(t) - x_i(t - \Delta t)|. \quad (16)$$

In the reported simulation, the weights were set to prioritize temperature safety over switching minimization. The temperature violation term therefore acts as the primary criterion, whereas the switching term is used to avoid unnecessary abrupt changes in cooling mode.

The values of w_1 and w_2 should be treated as simulation parameters. In the baseline scenario, $w_1 > w_2$ was assumed so that maintaining the admissible temperature range had priority over reducing switching frequency.

The value of $S(t)$ increases when the cooling mode changes in a given zone. Since the modes are encoded as ordered discrete levels, the component penalizes not only the occurrence of a switch, but also its magnitude. A transition from Low to Medium is therefore less penalized than a direct transition from Low to High. In practice, this supports the stabilization of control actions and reduces abrupt changes in cooling intensity, which is consistent with the behaviour expected in real refrigeration systems. Excessive switching may reduce operational stability and lead to temperature oscillations.

3.5. Formal Description of the EHO Modification

In the proposed model, EHO is used as a mechanism for selecting discrete control decisions (x(t)) for the three zones on the basis of current sensor data. The modification consists of three elements: (i) adapting the search space to a discrete form, (ii) evaluating candidate decisions using a one-step temperature-response model, and (iii) incorporating a switching penalty to reduce abrupt changes in cooling modes. In practice, after the positions of individuals are updated according to the clan mechanism, the continuous solutions are projected onto the space of admissible decisions:

$$x_i(t) = \Pi_{\{0,1,2\}}(\widetilde{x}_i(t)), \quad (17)$$

where $\widetilde{x}_i(t)$ denotes the value generated by the EHO update rules, and $\Pi_{\{0,1,2\}}$ is the projection operator that maps this value to the nearest admissible discrete level. Then, the value of F(x(t)) is calculated for each individual, and the best solution in the population determines the vector of control decisions for the given time iteration.

The modified EHO procedure used for the multi-zone control problem can be summarized as follows.

Pseudocode—modified EHO for multi-zone temperature control

1. Define simulation parameters: number of zones, number of sensors, time horizon, time step, temperature range, cooling modes, population size, number of clans, and maximum number of iterations.
2. Initialize the temperature state of each zone and assign sensors to zones.
3. For each time step t:
4. Aggregate sensor readings into zone-level temperatures $T_i(t)$.
5. Initialize the EHO population, where each individual represents a candidate vector $x(t) = [x_1(t), x_2(t), x_3(t)]$.
6. Divide the population into clans.
7. For each EHO iteration:
8. Identify the best individual in each clan.
9. Update non-best individuals using the clan-update mechanism.

10. Apply the migration mechanism to selected individuals.
11. Project continuous candidate values onto the discrete set $0, 1, 2$.
12. Evaluate each candidate using $F(x(t))$.
13. Preserve the best candidate solution.
14. Select the best vector $x^*(t)$ as the cooling-mode decision for the current time step.
15. Update the simulated temperature state and store temperature values, cooling modes, and performance indicators.
16. Continue until the full simulation horizon is completed.

3.6. Configuration of the Simulation Experiment and Organization of Input Data

The simulation experiment was designed to ensure comparability between successive simulation runs and consistency in the structure of input data. Each run covered a time horizon of 336 h, representing multi-day maritime transport, with a time step of $\Delta t = 0.5\ h$. This corresponded to 672 decision iterations, during which both temperature readings and cooling mode decisions were recorded.

The baseline simulation used 672 time steps, corresponding to 336 h with a 0.5 h sampling interval. The EHO configuration consisted of 3 clans, 5 individuals per clan, and 50 internal iterations per decision step. The total number of virtual sensors was 12, with four sensors assigned to each zone. Cooling modes were encoded as 0 = Low, 1 = Medium, and 2 = High. The reported example dataset contains the time stamp, zone temperatures, selected cooling modes, sensor energy values, and sensor transmission frequencies for each time step.

Because the present study is simulation-based, random disturbances affect the exact temperature trajectories and switching sequences. For this reason, the results should be interpreted in terms of aggregate behaviour and control patterns rather than as deterministic predictions of a specific physical container. In the revised version, the selected simulation cases are treated as illustrative examples, while the summary indicators are used to support the conclusions quantitatively.

The model included three independent temperature zones, reflecting spatially differentiated thermal conditions within the container cargo space. A network of virtual IoT sensors was distributed across the zones, comprising twelve temperature sensors in total. At each time step, sensor data were aggregated and used to evaluate the objective function and update the control decisions generated by EHO.

The cooling system was represented as a set of discrete operating modes corresponding to different levels of heat exchange intensity. Three control levels were adopted: Low, Medium, and High. Each mode could be activated independently in each zone, which allowed the model to capture local system responses to temperature variability and to analyse the temporal dynamics of switching between cooling levels.

To assess the stability of the algorithm and its sensitivity to the stochastic character of the population, multiple independent simulation runs were performed using the same experimental configuration. Each run used the same input data structure, number of sensors, time horizon, and definition of cooling modes. This made it possible to compare temperature dynamics and control strategies directly across successive simulation runs.

4. Research Results and Simulation Analysis

The simulation experiments included a series of independent runs of the EHO algorithm in a three-zone environment representing the conditions of temperature-sensitive cargo transport. Each run covered a horizon of 336 h, with a time step of $\Delta t = 0.5\ h$, corresponding to 672 decision iterations. The same model structure was maintained in all simulations: three independent temperature zones, twelve virtual IoT sensors in total, and

three discrete operating modes of the cooling system: Low, Medium, and High. The results were analysed at two levels. The first concerned temperature trajectories in individual container zones, which made it possible to assess the dynamics of thermal changes over time. The second concerned control maps, which present the sequences of control decisions made by EHO. Combining these two types of data made it possible to assess not only whether the temperature remained within the admissible range, but also how the algorithm selected cooling intensity in response to local changes in conditions.

To reduce reliance on graphical interpretation alone, the revised analysis uses the following quantitative indicators: mean temperature, standard deviation, minimum and maximum temperature, percentage of time within the admissible range, number of cooling-mode switches, share of Low/Medium/High operation, and total temperature violation magnitude. The total violation magnitude is defined as:

$$V = \sum_t \sum_{i=1}^{3} [\max(0, T_i(t) - 8) + \max(0, -T_i(t))] \quad (18)$$

A lower value of V indicates better compliance with the pharmaceutical temperature range. The number of mode switches is used as a proxy indicator of control stability, while mode shares indicate whether stabilization was achieved through continuous high-intensity cooling or through local corrective decisions.

4.1. Temperature Dynamics and Control Decisions

The analysis of time series indicates clear differences in temperature dynamics between the zones. In most simulations, changes did not occur simultaneously in all parts of the container. This confirms the asynchronous character of the system and the local response of EHO to temperature deviations. The algorithm did not introduce a single common correction for the entire cargo space. Instead, it differentiated control decisions according to the conditions observed in each zone.

The zones exhibited different behavioural patterns. In some runs, zone 0 showed a larger amplitude of variation, with transitions between extreme values. Zone 1 more often exhibited phases of gradual temperature increase or decrease, indicating smoother control dynamics. In selected simulations, zone 2 showed more stable trajectories, although short-term instability episodes also occurred and required rapid correction of the cooling mode. These differences support the adoption of a multi-zone system, as each part of the container may require a different regulatory response.

The control maps show that switching between the Low, Medium, and High modes was also local in character. In most cases, no sustained, simultaneous transition of all zones to the highest cooling level was observed. The High mode appeared rather as a corrective response in selected zones and in specific parts of the time horizon. This means that EHO did not treat the container as a homogeneous thermal space, but selected cooling intensity according to the local temperature trajectory.

4.2. Comparison of Trajectories Across Simulations

The comparison of successive simulations shows that the general operating pattern of the system was repeatable, while local temperature trajectories and cooling mode sequences differed between runs. Although the experimental configuration remained identical, individual simulations varied in the timing of Medium and High mode activation, the duration of stabilization periods, and the intensity of corrective actions. This variability results from the stochastic nature of EHO and from the algorithm's local response to changing sensor data.

The most stable trajectories occurred when temperature changes were distributed relatively evenly over time and cooling mode transitions took the form of short corrective

interventions. By contrast, longer periods of operation in Low mode could be followed by a temperature increase, requiring a transition to Medium or High mode. This did not, however, indicate a global change in the control strategy. In most cases, increased cooling intensity concerned only selected zones, which confirms the distributed character of decisions made by EHO.

The results indicate that the proposed model makes it possible to analyze not only temperature values, but also the structure of control decisions. This is important because, in IoT-based systems, maintaining temperature within the required range does not by itself explain how the control process operates. Only the combined analysis of temperature trajectories and control maps makes it possible to determine whether stabilization results from a uniform increase in cooling intensity or from locally differentiated system responses.

5. Simulation Runs

This section presents selected simulation runs that illustrate the behaviour of the proposed multi-zone temperature control model. Each case includes descriptive temperature statistics, the structure of cooling modes, temperature trajectories, and the corresponding control map. The purpose of this section is to show how EHO adjusts cooling decisions in response to local thermal conditions in individual container zones.

The detailed simulation runs presented below should be treated as representative examples illustrating different operating conditions and control responses observed in the proposed EHO-based multi-zone system.

The descriptive temperature statistics indicate differentiated dynamics across the zones. The highest variability was recorded in Zone 1, where the standard deviation reached $\sigma = 2.38$ °C. Zone 2 showed a relatively lower standard deviation, $\sigma = 1.57$ °C, which suggests a more stable thermal trajectory in this simulation run.

The structure of cooling mode shares indicates the dominance of Low mode in Zone 0 and increased Medium mode activity in Zone 2. The number of switches suggests the local character of EHO control decisions.

The trajectories shown in Figure 1 confirm the asynchronous character of temperature changes between the zones. Temperature responses are time-shifted, which indicates that EHO adjusts cooling intensity locally rather than through a single global correction. The highest variability is observed in Zone 1, while Zone 2 shows a more stable trajectory with shorter episodes of abrupt change. Zone 0 exhibits periodic transitions between extreme values, which is consistent with the dominance of Low mode and less frequent control interventions presented in Tables 2 and 3. Overall, the results indicate distributed control, in which each zone is regulated independently according to its local thermal conditions.

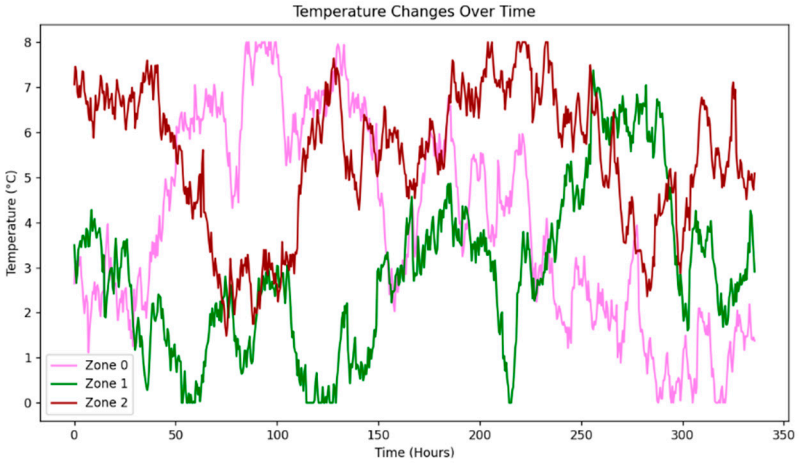


Figure 1. Temperature changes in the three container zones in simulation run 1.

Table 2. Descriptive temperature statistics for simulation run 1 (time horizon: 336 h; Delta t = 0.5 h; $N = 672$).

Zone	Mean [°C]	Std. Dev. [°C]	Min [°C]	Max [°C]
Zone 0	2.21	2.07	0.00	8.00
Zone 1	4.29	2.38	0.00	8.00
Zone 2	4.11	1.57	0.00	8.00

Table 3. Structure of cooling modes and number of mode switches in simulation run 1 ($N = 672$).

Zone	Low (Time Share)	Medium (Time Share)	High (Time Share)	Number of Mode Switches
Zone 0	74.0%	17.3%	8.8%	20
Zone 1	36.0%	31.0%	33.0%	40
Zone 2	23.8%	65.0%	11.2%	72

The control map shows changes in the operating modes of the cooling system across the three container zones over the full 336-h simulation horizon. The colours correspond to three levels of cooling intensity: Low, Medium, and High. This visualization makes it possible to assess not only the share of individual modes, but also their temporal distribution and the switching pattern between control levels. In Zone 0, Low mode clearly dominates, which is consistent with Table 3, where its share reaches 74.0%. Short episodes of transition to Medium and High indicate that EHO does not maintain a constant cooling intensity, but applies local corrective responses. Zone 1 shows a more balanced distribution of the three modes, which corresponds to the higher temperature variability reported in Table 2. In this zone, longer periods of Low mode are accompanied by frequent transitions to Medium and High, indicating more active regulation under variable local conditions. The highest switching dynamics are observed in Zone 2, where the number of mode changes reaches 72. The dominance of Medium mode, supported by periodic transitions to High, suggests more intensive but still locally adjusted regulation. The absence of simultaneous switching across all zones confirms the distributed character of control. The system does not follow a single global command for the entire container, but selects the cooling level separately for each zone on the basis of its current thermal state. The control map therefore complements the analysis of temperature trajectories. Figure 1 shows the thermal response of the system, while Figure 2 Control Map 1 reveals the control decisions that produced the observed temperature pattern. Taken together, both visualizations show that the proposed EHO variant performs local and adaptive temperature regulation in a multi-zone environment, without enforcing full synchronization of the cooling system.

The analysis of the trajectories shown in Figure 3 indicates a clearly asynchronous pattern of temperature changes across the three container zones in simulation run 2. Zone 0 shows the largest amplitude fluctuations, with periods of rapid temperature increase in the middle and final phases of the simulation. This suggests more frequent cooling mode adjustments in response to local environmental disturbances. Zone 1 exhibits smoother dynamics, with distinct phases of gradual cooling followed by renewed temperature increase. This may be interpreted as an effect of the adaptive operation of the EHO clan mechanism. Zone 2, by contrast, shows relatively higher short-term instability, visible in numerous episodes of rapid temperature drops in the second half of the simulation horizon. The asynchronous behaviour of the zones confirms the local response of the algorithm to environmental disturbances and the absence of a globally imposed control

strategy. This distributed mode of operation supports temperature stabilization over the long simulation horizon.

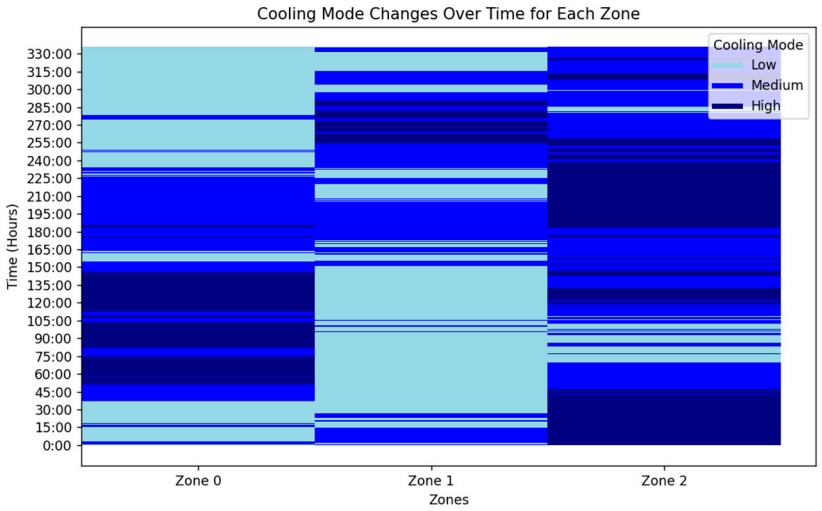


Figure 2. Control Map 1. Temporal distribution of cooling modes in the three container zones in simulation run 1.

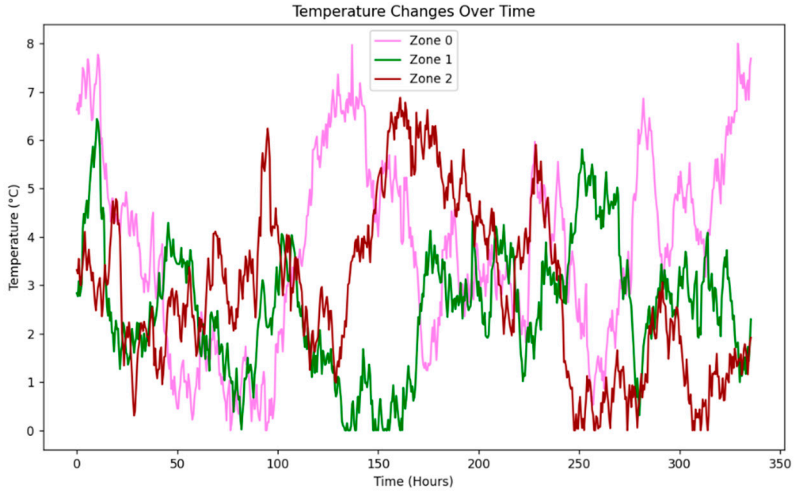


Figure 3. Temperature changes in the three container zones in simulation run 2, showing clear trajectory asynchrony.

The control map presents the sequence of control decisions made by EHO in simulation run 2. The switching pattern confirms the local character of control, as the zones do not change operating modes simultaneously. In Zone 0, longer periods of Low mode are interrupted by Medium segments and shorter High episodes. This indicates pointwise increases in cooling intensity in response to local temperature rises.

Zone 1 in Figure 4. Control Map 2 shows a more variable control pattern, including both longer Low-mode periods and sequences of transitions to Medium and High. Numerous short switches are visible especially in the final part of the simulation horizon, which may indicate greater sensitivity of this zone to local temperature deviations. Zone 2 shows longer Low-mode segments in the initial and final phases, with clear activation of Medium mode in the middle part of the run. Periodic transitions to High have a corrective character and do not lead to sustained dominance of the highest cooling level.

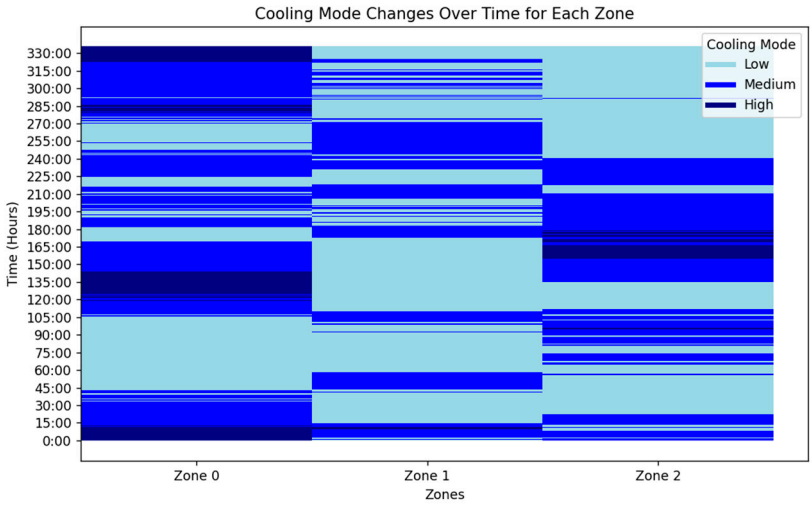


Figure 4. Control Map 2. Temporal distribution of cooling modes in the three container zones in simulation run 2.

The absence of global switching synchronization confirms that EHO does not control the container as a homogeneous thermal space. Control decisions are made separately for each zone, according to its local temperature dynamics. The control map complements the interpretation of Figure 3 by showing that the observed trajectory asynchrony results from a distributed selection of cooling modes, rather than from random system instability.

The trajectories shown in Figure 5 indicate clearly differentiated temperature dynamics across the three container zones in simulation run 3. Zone 2 reaches the highest temperature values in the first half of the time horizon, with prolonged periods in the upper part of the admissible range. This may indicate limited cooling intensity in the initial phase of the simulation. In the later part, a gradual temperature decrease is observed, suggesting adaptive adjustment of the EHO control strategy.

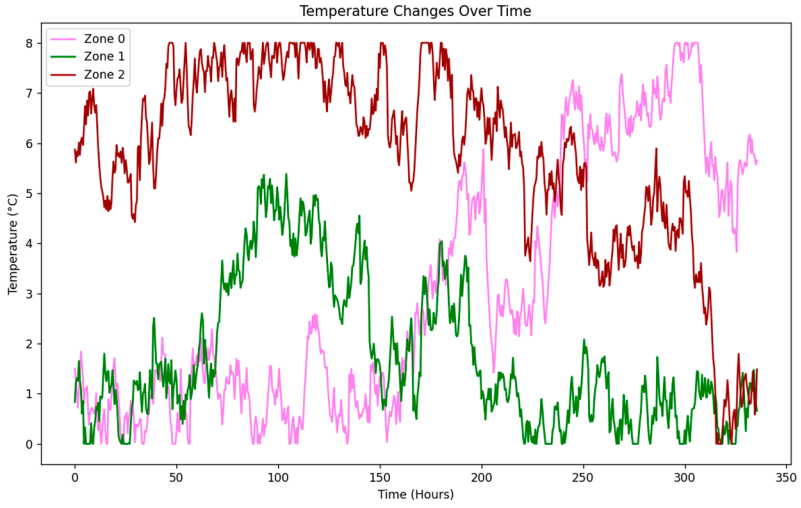


Figure 5. Temperature changes in simulation run 3, with prolonged operation in the upper temperature range.

Zone 1 shows relatively low temperature values and a higher number of short-term fluctuations. Episodes of rapid cooling below average values are followed by a gradual return to a stable range. This may indicate local operation of the clan mechanism, leading to more frequent cooling mode corrections in response to sensor data variability.

The largest amplitude of change in the second half of the simulation is observed in Zone 0, where a clear upward temperature trend and abrupt transitions between extreme values occur. The absence of simultaneous synchronization between the zones confirms the local character of control decisions. EHO does not enforce global changes in cooling parameters, but adjusts regulation levels individually for each zone. This supports system stabilization over the long simulation horizon and limits excessive mode switching.

The control map presents the sequence of control decisions made by EHO in simulation run 3. In Zone 0, Low mode predominates, covering approximately 59% of the simulation horizon, with a supplementary share of Medium mode and a clear but time-limited use of High mode. This pattern indicates periodic intensification of cooling, especially in the final part of the run, where longer segments of higher regulation levels are visible. Zone 1 shows the most stable control profile. Low mode covers approximately 77% of its operating time, while Medium mode appears mainly in the middle part of the horizon. High mode occurs only incidentally. This means that, despite the observed temperature fluctuations, the algorithm did not require prolonged activation of the highest cooling intensity in this zone. The control decisions were closer to moderate corrections than to abrupt interventions. A different pattern is observed in Zone 2, where High mode dominates, covering approximately 56% of the simulation horizon. Medium mode accounts for about 36%, while Low mode appears only in shorter segments. This distribution is consistent with Figure 5, where Zone 2 remained for an extended period in the upper part of the admissible temperature range. The control map therefore shows that EHO responded to this situation by increasing cooling intensity, especially in the first and middle parts of the simulation. The comparison of the three zones confirms the absence of global synchronization. At the same time, one zone may remain in Low mode while another requires High mode. This indicates that EHO performs local control adapted to the differentiated thermal dynamics of individual container areas. Figure 6 Control Map 3 complements Figure 5 by showing that prolonged operation in the upper temperature range does not lead to a uniform increase in cooling intensity across the whole system, but to selective regulation of selected zones.

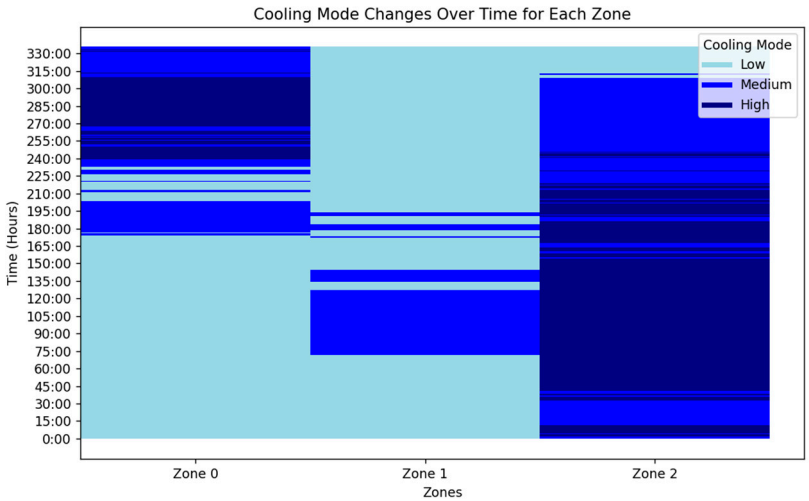


Figure 6. Control Map 3. Temporal distribution of cooling modes in the three container zones in simulation run 3.

The trajectories shown in Figure 7 indicate strongly differentiated temperature dynamics across the three container zones in simulation run 4. Zone 0 shows clear phases of maintaining temperature in the upper part of the admissible range during the initial phase. These are followed by gradual decreases and periods of instability in the final part

of the time horizon. This may indicate an initially stabilizing control strategy, followed by increased adaptiveness later in the simulation.

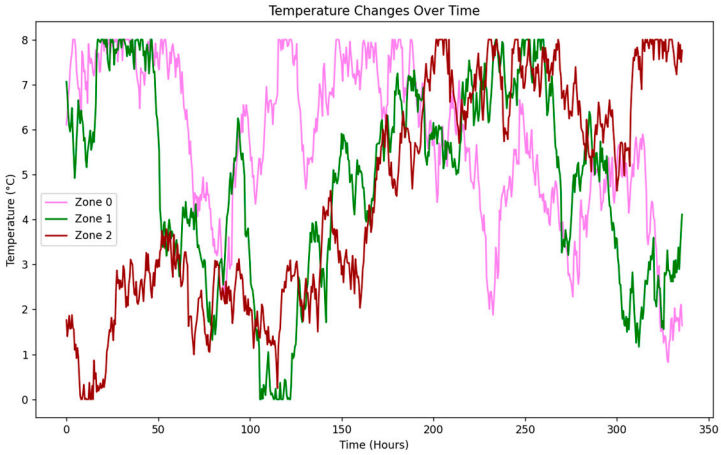


Figure 7. Temperature changes in simulation run 4, with episodes of abrupt corrections in the middle zone.

Zone 1 exhibits the highest short-term variability, visible in abrupt transitions between extreme values. This includes episodes of rapid cooling around the middle part of the simulation. Such behaviour suggests more intensive local adjustments of the cooling mode, resulting from the response of EHO to dynamic changes in sensor data.

Zone 2 shows a clear upward temperature trend, especially in the second half of the simulation horizon, where long periods close to the upper boundary of the admissible range are observed. This may indicate a gradual shift in the control strategy towards increased cooling intensity in response to accumulating temperature deviations. The absence of synchronization between zones confirms the decentralized character of control decisions. EHO does not impose a global change in the cooling system mode, but adjusts regulation levels locally. This helps limit simultaneous system loads and supports temperature stabilization over the long time horizon.

The control map shows a clearly differentiated pattern of control decisions made by EHO across the three container zones in simulation run 4. In Zone 0, High mode predominates, especially in the initial and middle parts of the simulation horizon. It can be estimated to cover more than half of the operating time in this zone. Medium mode appears mainly in the final part of the simulation, while Low mode occurs only episodically. This distribution indicates a prolonged need for intensive cooling, consistent with Figure 7, where Zone 0 periodically remained in the upper part of the admissible temperature range. Zone 1 presents a more balanced but still dynamic control profile. Long segments of High mode are visible in the initial and middle parts of the run, followed by transitions to Medium and Low. The middle section is particularly important, as it contains numerous switches between regulation levels. This pattern corresponds to the episodes of abrupt correction identified in the temperature analysis and indicates an intensive local system response to short-term variability in sensor data. In Zone 2, Low mode initially predominates. Later in the simulation, however, there is a clear shift towards Medium and High modes. The highest cooling level becomes dominant especially in the final phase of the time horizon. This can be interpreted as a response to the increasing temperature trend observed in this zone. The control map therefore shows a change in the regulatory strategy: from limited intervention in the initial period to intensified cooling in the second half of the simulation. The comparison of the three zones confirms the distributed character of system operation. EHO does not impose simultaneous cooling mode changes across the entire container. Instead, it differentiates decisions according to the local temperature

trajectory. Figure 8 Control Map 4 complements Figure 7 by showing that the abrupt correction episodes in the middle zone are not part of a global system response, but result from local adjustment of the cooling level to the temporary dynamics of that zone.

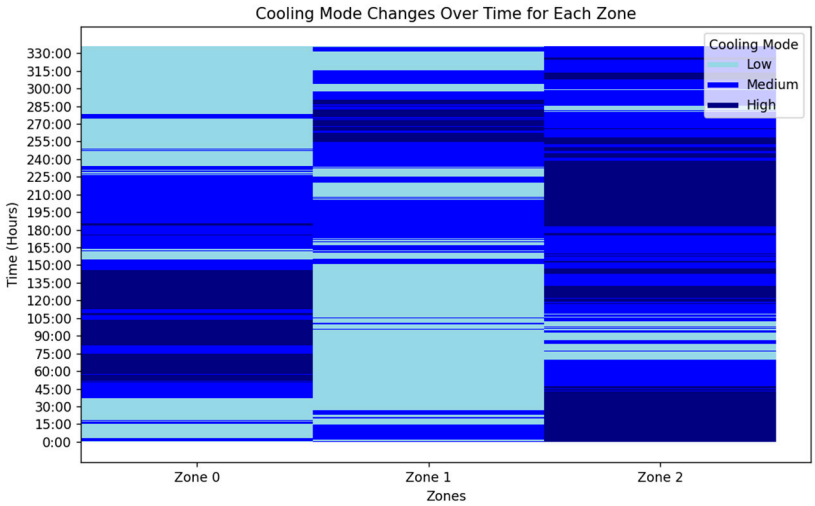


Figure 8. Control Map 4. Temporal distribution of cooling modes in the three container zones in simulation run 4.

The trajectories shown in Figure 9 indicate a clearly asynchronous pattern of temperature changes across the three container zones in simulation run 5. Zone 1 shows the highest short-term instability, with numerous episodes of rapid cooling towards values close to the lower boundary of the admissible temperature range. These episodes are particularly visible in the middle and final phases of the simulation, suggesting intensive local responses of EHO to dynamic changes in input data. Zone 0 presents a more wave-like trajectory, with periods of gradual temperature increase interrupted by shorter stabilization phases. In the second half of the simulation horizon, the amplitude of changes becomes more pronounced, which suggests adaptive adjustment of the control strategy in response to longer-term temperature deviations. Zone 2, in turn, is characterized by alternating phases of temperature increase and decrease, including prolonged periods in the upper part of the admissible range and short episodes of rapid drops that may result from temporary cooling intensification. The absence of simultaneous changes across all zones confirms the decentralized character of control decisions. EHO applies a local control strategy in which individual zones respond independently to environmental variability. This supports the limitation of excessive mode switching and contributes to temperature stabilization over the long time horizon.

The control map indicates a strongly differentiated distribution of control decisions across the three container zones. In Zone 0, Low, Medium, and High modes alternate over time, with the highest concentration of higher cooling levels occurring in the middle part of the simulation horizon. High mode appears there in longer blocks, suggesting a periodic need for intensive regulation. In the final part of the simulation, the system returns to Low mode, which may indicate stabilization of local thermal conditions.

Zone 1 is characterized by high variability in control decisions. High mode initially predominates, followed by sequences of Medium mode and longer Low-mode segments. This pattern corresponds to the episodes of rapid cooling described in Figure 9. It confirms that EHO responded intensively in this zone, but did not maintain the highest cooling level continuously. The decisions had a corrective character and were adjusted to short-term temperature fluctuations.

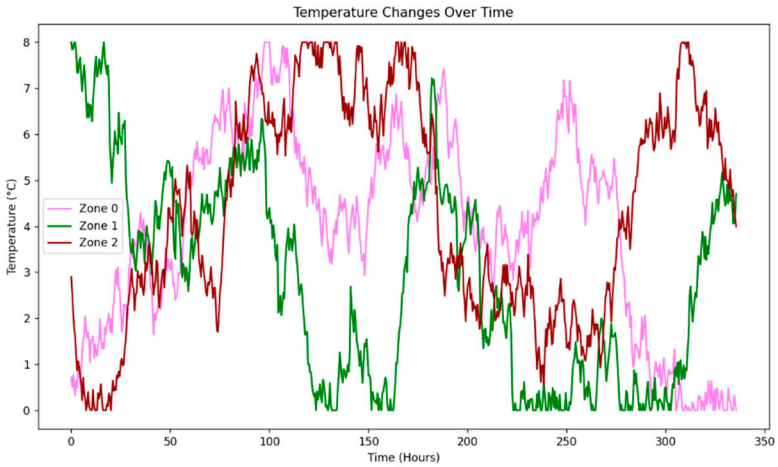


Figure 9. Temperature changes in simulation run 5, with intensified short-term fluctuations.

In Zone 2, long periods of High mode are visible, especially in the middle part of the run, interspersed with Medium and Low segments. This can be interpreted as a response to temperature remaining in the upper part of the admissible range. At the same time, short transitions to lower modes indicate that the algorithm did not lead to sustained overloading of the cooling system, but graded the intensity of regulation according to current conditions.

The comparison of the three zones confirms the absence of simultaneous control of the entire container. Each zone shows a different switching rhythm, and periods of High-mode operation do not permanently overlap across all system areas. Figure 10 Control Map 5 complements Figure 9 by showing that intensified short-term fluctuations do not result from chaotic system operation, but from locally differentiated EHO decisions adapted to the changing temperature dynamics in individual zones.

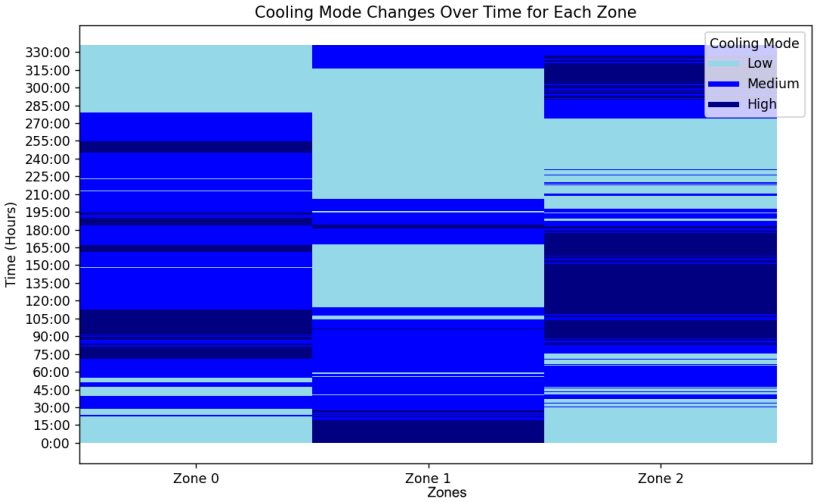


Figure 10. Control Map 5. Temporal distribution of cooling modes in the three container zones in simulation run 5.

The trajectories shown in Figure 11 indicate strongly differentiated temperature dynamics across the three zones of the cooling system. Zone 0 maintains a relatively high temperature level for a substantial part of the simulation horizon, with visible stabilization periods in the upper part of the admissible range. This may indicate a limited number of intensive control interventions.

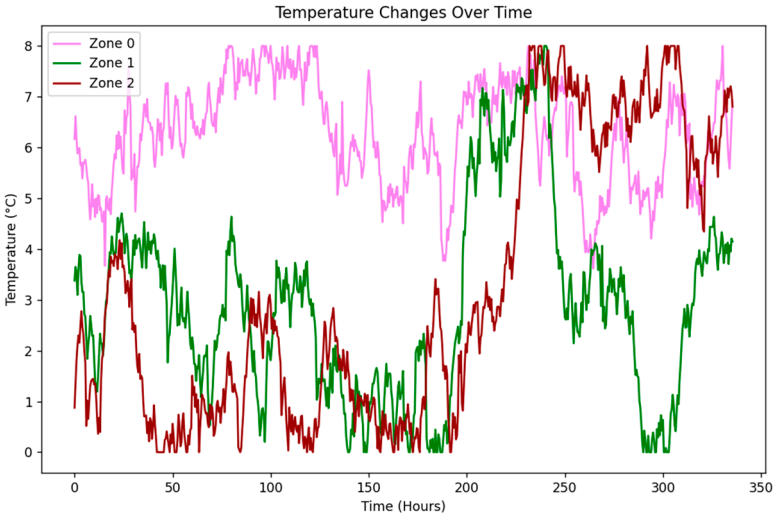


Figure 11. Temperature changes in simulation run 6, with an elevated temperature level in Zone 0.

Zone 1 shows a more variable trajectory, including both episodes of deep cooling and phases of gradual temperature increase. This remains consistent with the local control character attributed to the EHO clan mechanism. The highest short-term instability is observed in Zone 2, where abrupt transitions between low and high temperature values occur, especially in the second half of the simulation.

The visible asynchrony between the zone trajectories suggests the absence of global synchronization and confirms local control decision-making. The differences in amplitude and fluctuation frequency indicate distributed cooling control, which allows the system to respond adaptively to changing environmental conditions without enforcing simultaneous changes across the entire system. This operating pattern may support long-term system stability by limiting sudden, coordinated loads on the cooling system.

Figure 12 Control Map 6 indicates a clear asymmetry in control decisions between the zones. In Zone 0, High mode predominates over a substantial part of the simulation horizon, especially in its middle segment. Medium mode appears mainly in the initial and final parts of the trajectory, while Low mode occurs only marginally. This pattern is consistent with Figure 11, where Zone 0 maintained a relatively elevated temperature level and therefore required more frequent activation of intensive cooling.

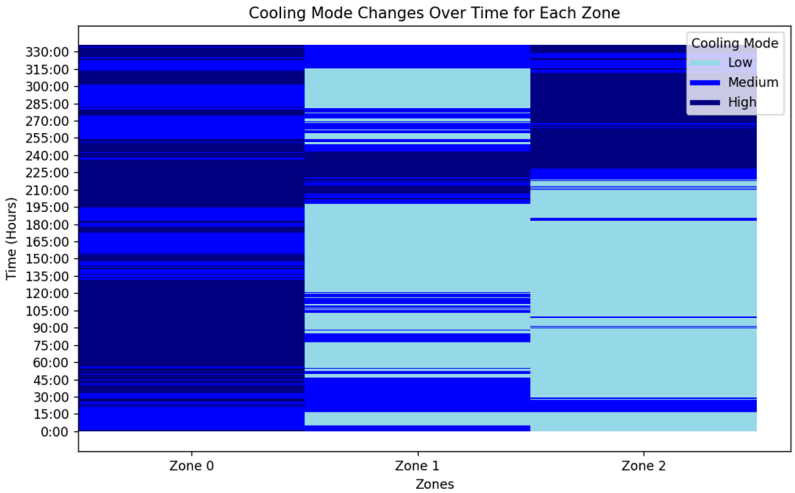


Figure 12. Control Map 6. Temporal distribution of cooling modes in the three container zones in simulation run 6.

Zone 1 shows a more differentiated control profile. Alternating segments of Low, Medium, and High modes are visible, with the highest cooling intensity occurring mainly in the middle part of the simulation. Longer Low-mode periods indicate, however, that EHO did not maintain increased regulation continuously, but switched the system according to local temperature dynamics. This corresponds to a trajectory that included both cooling episodes and later phases of temperature increase.

In Zone 2, Low mode predominates, particularly in the first and middle parts of the time horizon. In the final segment, however, a clear activation of High mode is visible, preceded by periods of Medium-mode operation. This can be interpreted as a response to increasing short-term instability and abrupt temperature transitions observed in this zone. The regulation therefore takes the form of a delayed but intensive correction.

Figure 12 Control Map 6 confirms the absence of a uniform operating pattern for the entire cooling system. While Zone 0 requires intensive cooling, Zone 2 remains in Low mode for an extended period, and Zone 1 passes through sequences of intermediate regulation. This means that EHO differentiates control decisions according to the local state of each zone. Combined with Figure 11, the map shows that an elevated temperature level in one part of the container does not lead to global cooling intensification, but to selective adjustment of the operating mode.

The trajectories shown in Figure 13 indicate a clearly asynchronous pattern of temperature changes between the zones of the cooling system. Zone 0 initially shows low temperature values, followed by a gradual increase and stabilization in the upper part of the admissible range. This suggests limited regulation intensity in the middle part of the simulation horizon.

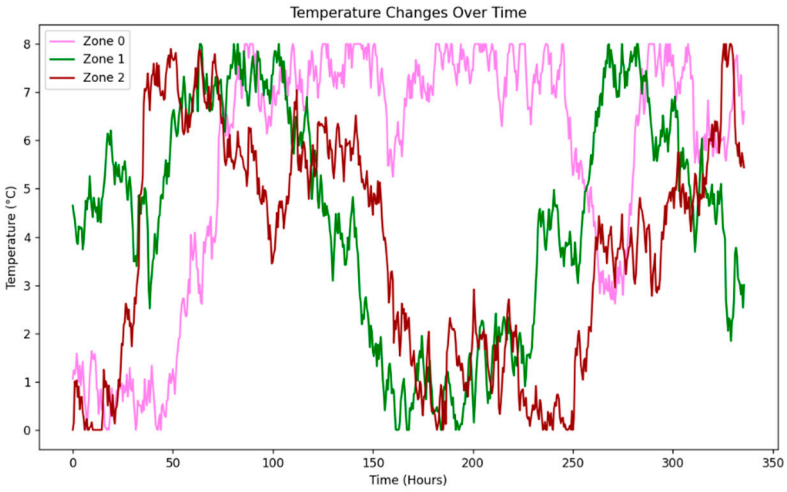


Figure 13. Temperature changes in simulation run 7 with Zone 0 transitioning from low to high values.

Zone 1 exhibits more complex dynamics, including phases of abrupt cooling and later periods of temperature increase. This remains consistent with the local decision-making character of the EHO clan mechanism. Zone 2 shows greater short-term variability, with visible episodes of rapid transitions between extreme temperature levels, especially in the initial and final parts of the simulation.

The absence of simultaneous temperature changes across the three zones indicates distributed cooling control, in which regulatory decisions are made locally without global synchronization. Differences in the amplitude and frequency of temperature fluctuations between zones may help limit sudden overloads of the cooling system and support its stabilization over the long time horizon.

Figure 14 Control Map 7 presents the pattern of EHO control decisions corresponding to the temperature trajectory in simulation run 7. In Zone 0, a transition is visible from lower

regulation intensity in the initial part of the horizon to a higher share of Medium and High modes later in the run. This distribution is consistent with Figure 13, where temperature increases from low values to levels close to the upper boundary of the admissible range. The algorithm does not respond with a single global correction, but gradually increases cooling intensity in this zone.

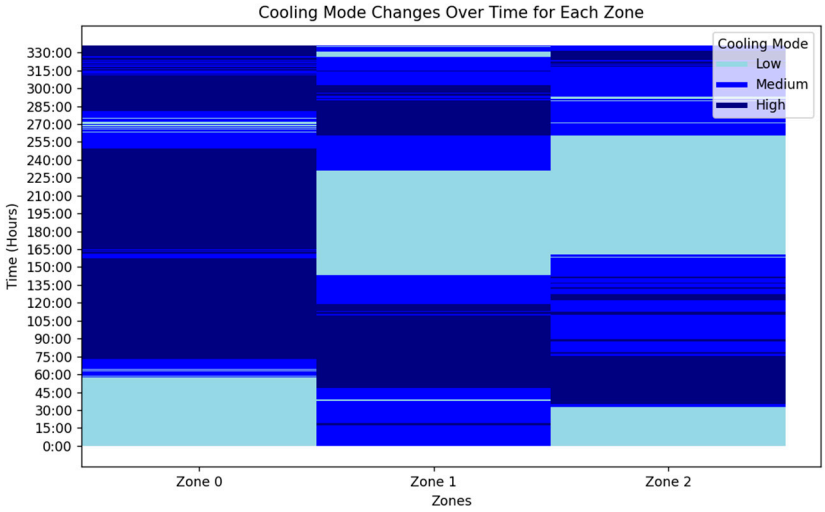


Figure 14. Control Map 7. Temporal distribution of cooling modes in the three container zones in simulation run 7.

Zone 1 shows a more variable control profile. Switches between Low, Medium, and High modes occur in several parts of the time horizon, indicating local correction of temperature instability. This pattern corresponds to the phases of abrupt cooling and later temperature increase described in the analysis of Figure 13. Regulation is not based on continuous operation in High mode, but on sequences of corrections adjusted to the current state of the zone.

Zone 2 shows the highest short-term variability in control decisions. Frequent transitions between regulation levels, especially in the initial and final parts of the simulation, indicate EHO responses to rapid temperature changes. High mode appears periodically as a response to local deviations, while the presence of Low and Medium modes shows that the system does not maintain maximum cooling intensity continuously.

Figure 14 Control Map 7 confirms the distributed character of system operation. Each zone follows a different switching rhythm, and the temperature change in Zone 0 does not automatically increase cooling intensity across the entire container. Combined with Figure 13, the map shows that EHO performs local adaptation of operating modes, reducing the need for global synchronization and enabling selective responses to different temperature trajectories in individual zones.

The trajectories shown in Figure 15 indicate clear differences in temperature dynamics across the three zones of the cooling system. Zone 0 initially shows an elevated temperature level, followed by a period of rapid cooling in the middle part of the simulation horizon and a later phase of gradual stabilization.

Zone 1 exhibits relatively smooth dynamics, with long periods of temperature remaining in the middle range and occasional transitions to higher values. This is consistent with the local character of control attributed to the EHO clan mechanism. Zone 2 shows a more unstable short-term trajectory, with numerous episodes of temperature drops towards the lower boundary of the admissible range, followed by a gradual increase in the final phase of the simulation.

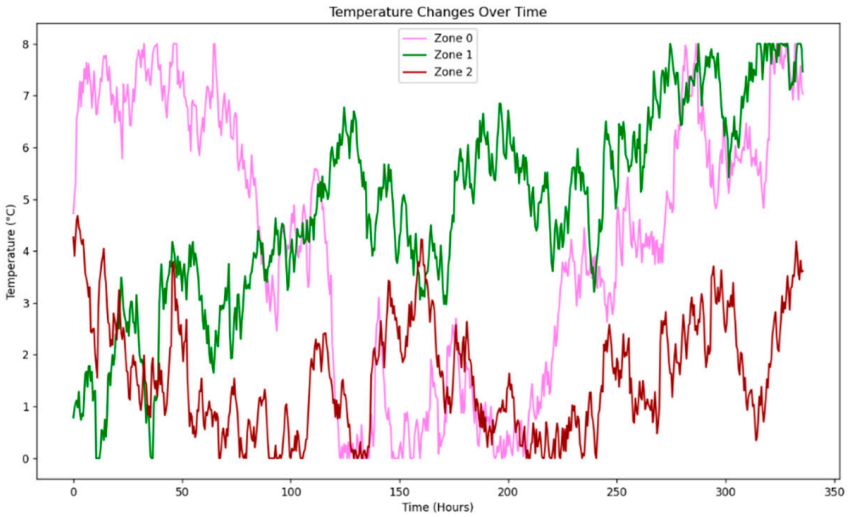


Figure 15. Temperature changes in simulation run 8, with an episode of intensive cooling in the middle phase.

The absence of simultaneous temperature changes across the zones indicates the distributed character of control decisions. The asynchrony of the trajectories and the differentiated amplitude of fluctuations suggest local adaptation of the cooling strategy. This helps limit sudden coordinated loads on the system and supports temperature stabilization over the long time horizon.

The control map shows a differentiated pattern of EHO control decisions in simulation run 8. In Zone 0, long periods of High mode are visible in the initial part of the horizon, followed by a transition to Low mode in the middle phase. This pattern corresponds well to the intensive cooling episode described in Figure 15. After a period of high cooling intensity, regulation is reduced, which may indicate a system response to the attainment of lower temperature values.

Zone 1 is characterized by the largest share of Medium mode, particularly in the middle part of the simulation. High mode appears mainly in the final segment of the horizon, whereas Low mode occurs in shorter periods at the beginning and at selected later points. This control profile corresponds to the smoother temperature dynamics, in which EHO does not enforce continuous operation at the highest level, but uses intermediate regulation as the dominant stabilization strategy.

In Zone 2, Low mode predominates and covers a substantial part of the simulation horizon, especially in the middle section. At the same time, short transitions to Medium and High are visible in the initial and final parts of the run. This indicates that, despite short-term temperature instability, the algorithm applied primarily limited cooling intensity in this zone, activating higher modes only as corrective actions.

Figure 16 Control Map 8 confirms the distributed character of regulation. While Zone 0 shifts from intensive cooling to Low mode, Zone 1 remains mainly under intermediate regulation and Zone 2 operates predominantly in Low mode. This comparison shows that EHO does not respond to the cooling episode by globally switching the entire system, but differentiates decisions according to local temperature trajectories. Combined with Figure 15, the map indicates that system stabilization results from selective zone regulation rather than uniform control of the entire container.

The trajectories shown in Figure 17 indicate a clearly asynchronous pattern of temperature changes across the three zones of the cooling system. Zone 0 initially shows elevated temperature values, followed by a gradual decrease in the middle part of the simulation horizon and a renewed increase in the final phase.

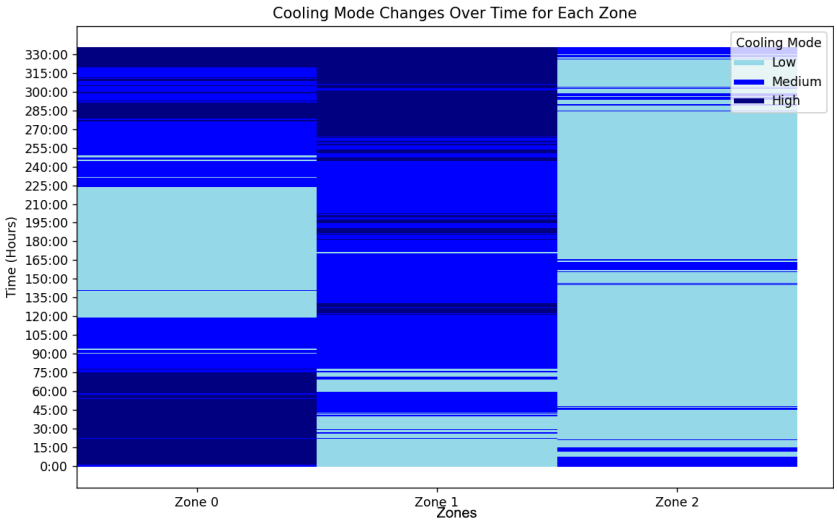


Figure 16. Control Map 8. Temporal distribution of cooling modes in the three container zones in simulation run 8.

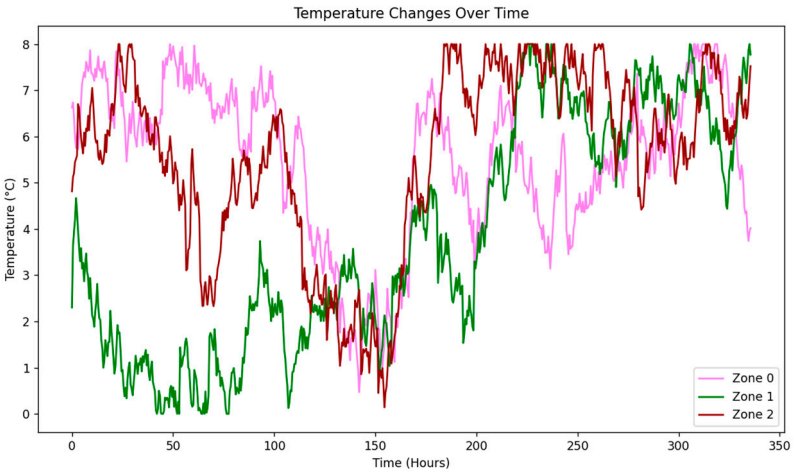


Figure 17. Temperature changes in simulation run 9, with a decreasing-then-increasing trend in Zone 0.

Zone 1 is characterized by pronounced dynamics, including periods of deep cooling interspersed with gradual temperature increases. This remains consistent with the local control character attributed to the EHO clan mechanism. Zone 2 shows relatively more stable temperature values in the initial phase, followed by episodes of increased variability, especially in the second half of the analysed time horizon.

The absence of simultaneous temperature changes across the zones confirms the distributed character of control decision-making. Differences in fluctuation amplitude and time shifts between trajectories indicate local adaptation of the cooling strategy. This reduces the need for global system synchronization and may support long-term operational stability.

The control map presents the pattern of EHO control decisions corresponding to the temperature trajectory in simulation run 9. In Zone 0, a substantial share of High mode is visible, especially in the initial and final parts of the time horizon. In the middle segment, longer periods of Low and Medium modes appear. This distribution corresponds well to the decreasing-then-increasing trend described in Figure 17: more intensive cooling in the first phase leads to a temperature decrease, while the later increase in the share of High mode reflects a response to rising temperature values in the final part of the simulation. Zone 1 is characterized by a clear transition between regulation phases. Low mode dominates in the first part of the run, followed by segments of Medium mode, while the share of High mode increases in the final part. This indicates gradual intensification

of control in response to changing local conditions. The pattern remains consistent with the observed periods of cooling and later temperature increase. EHO does not maintain a constant cooling intensity in this zone, but modifies the operating mode according to the local temperature trajectory.

In Zone 2, an opposite regulation sequence is visible. Transitions between Medium and High modes occur initially, followed by a longer period of Low mode, while the share of High mode increases again in the final part. This profile indicates the corrective character of control decisions. The algorithm responds to short-term deviations, but does not maintain maximum cooling intensity continuously.

Figure 18 Control Map 9 confirms the asynchronous character of system operation. Mode changes occur at different moments in individual zones, and periods of intensive regulation do not cover the entire container simultaneously. Combined with Figure 17, the map shows that the decreasing-then-increasing trend in Zone 0 does not result in a global change in strategy, but remains part of local control adaptation performed by EHO.

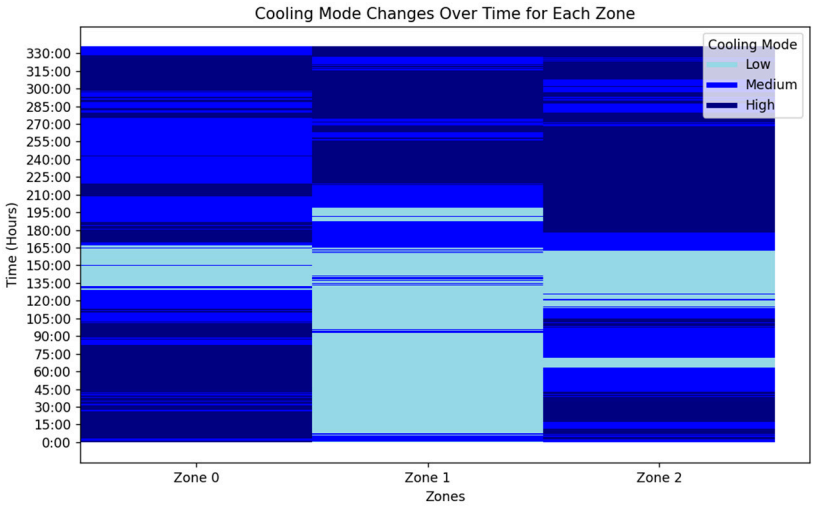


Figure 18. Control Map 9. Temporal distribution of cooling modes in the three container zones in simulation run 9.

The trajectories shown in Figure 19 indicate clearly differentiated temperature dynamics across the three zones of the cooling system. Zone 0 is characterized by episodes of low temperature values in the initial and middle parts of the simulation horizon, followed by a gradual increase and greater variability in the final phase of the run. Zone 1 exhibits the broadest amplitude fluctuations, including both phases of intensive cooling and periods of elevated temperature, which is consistent with the local control character attributed to the EHO clan mechanism. Zone 2, in turn, shows a trajectory with distinctly episodic dynamics, in which phases of stabilization are interspersed with more abrupt transitions between temperature levels. The absence of simultaneous temperature changes across all zones confirms the distributed character of control decisions. The asynchrony of the trajectories and the time shifts between temperature peaks indicate local adaptation of the cooling strategy, which reduces the need for global synchronization of system operation and may support long-term stability.

The control map presents a differentiated pattern of EHO control decisions in simulation run 10. In Zone 0, Low mode dominates for a substantial part of the initial and middle horizon, interrupted only by short transitions to Medium mode. A clear shift towards higher cooling levels appears only in the final part of the run, including longer segments of Medium and High modes. This pattern corresponds to the gradual temperature increase and growing variability observed in the final phase of Figure 19.

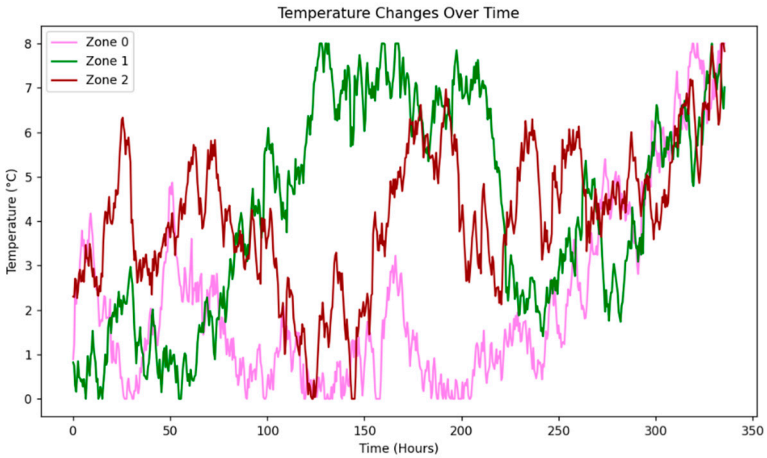


Figure 19. Temperature changes in simulation run 10, with increasing variability in the final part of the trajectory.

Zone 1 shows a more active regulation profile. Low mode predominates in the first part of the run, while a longer High-mode phase is visible in the middle segment, supported by transitions to Medium mode. This indicates intensified cooling in response to broad temperature fluctuations. Later in the horizon, regulation returns to lower and intermediate modes, suggesting a corrective rather than continuous use of the highest cooling intensity.

In Zone 2, the control pattern is episodic. Clear transitions between Low, Medium, and High modes are visible, with Medium and High occurring more frequently in the middle and final parts of the simulation. This distribution is consistent with Figure 19, where Zone 2 shows stabilization phases interspersed with more abrupt temperature transitions. EHO therefore responds to local changes by temporarily increasing cooling intensity, without maintaining the maximum operating level continuously.

Figure 20 Control Map 10 confirms the absence of global synchronization in control decisions. Zone 0 remains in Low mode for an extended period, while Zone 1 undergoes a phase of intensive cooling and Zone 2 shows sequences of shorter corrections. Combined with Figure 19, the map shows that increasing variability in the final part of the trajectory does not lead to a uniform response of the whole system, but to local differentiation of operating modes by EHO.

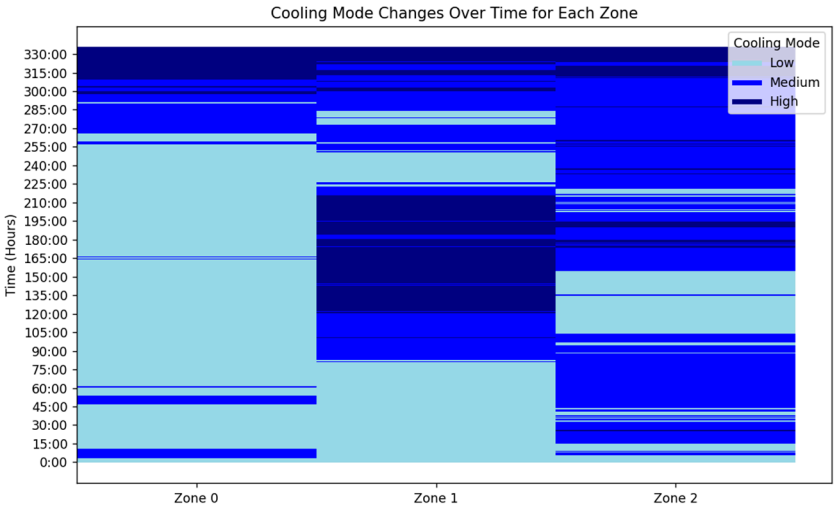


Figure 20. Control Map 10. Temporal distribution of cooling modes in the three container zones in simulation run 10.

6. Discussion and Conclusions

The simulation experiments made it possible to assess the modified EHO algorithm as a mechanism for temperature regulation in a multi-zone IoT environment. The results indicate that the proposed model does not operate as a uniform regulator of the entire cargo space. Instead, it functions as a system of local control decisions made separately for each container zone. This is important from the perspective of the cold chain, because real thermal conditions inside a container are not homogeneous. Individual areas may respond differently to solar radiation, insulation differences, their position relative to the refrigeration unit, cargo space opening, and local environmental disturbances. The analysis of temperature trajectories and the corresponding control maps confirmed the asynchronous character of system operation. Across successive simulations, the zones did not change temperature simultaneously, and cooling mode switches did not follow a single global pattern. This means that EHO differentiated control decisions according to local temperature trajectories rather than the averaged state of the entire container. In practice, one zone could remain in Low mode while another required Medium or High mode. This type of regulation is particularly important in multi-zone systems, as it reduces the risk of the entire system overreacting to a disturbance occurring only in one area. The results also show that decisions made by EHO were adaptive. In scenarios where temperature remained in the upper part of the admissible range, the share of Medium and High modes increased. In trajectories with episodes of rapid cooling, the algorithm reduced cooling intensity by switching to Low mode or by applying shorter corrective actions. This was especially visible in the control maps, which revealed the decision-making layer not directly visible in the temperature plots alone. The combined interpretation of both types of visualization showed that the observed temperature variability was not the result of random system instability, but the consequence of locally differentiated control decisions. An important result of the study is the confirmation that the multi-zone model can maintain temperature within the required range of 0–8 °C without continuously applying the highest cooling level in all zones. In the analysed trajectories, High mode most often appeared as a corrective response or as a temporary form of regulation intensification, rather than as a dominant global strategy. This means that the proposed control system may limit excessive activation of the cooling system while preserving the ability to respond to local temperature deviations. From the perspective of pharmaceutical transport, this is relevant both for the stability of transport conditions and for limiting abrupt changes in the operation of the technical system. At the interpretive level, the results indicate that the use of EHO in an IoT environment may support a shift from simple temperature monitoring to control based on local assessment of system state. In this model, sensors do not only perform a recording function. Their readings become the basis for control decisions that are updated in successive time steps and differentiated spatially. In this way, sensor data are transformed into control signals, while the IoT system ceases to function solely as an observation infrastructure. It becomes part of an active mechanism for maintaining the quality of transport conditions.

It should be emphasized that the results are simulation-based. The input data were generated synthetically in order to reproduce selected characteristics of maritime transport, including changing environmental conditions, asynchronous zone behaviour, and local temperature disturbances.

The model should therefore be interpreted as a computational proof-of-concept. It does not claim to reproduce the complete thermodynamics of a refrigerated container, the airflow generated by a specific refrigeration unit, the heat capacity and spatial arrangement of a real pharmaceutical cargo, or actuator response delays. The results demonstrate the

internal behaviour of the proposed control logic under controlled synthetic scenarios, but they do not yet constitute operational validation.

This approach made it possible to control the experimental structure and analyse algorithm behaviour across multiple comparable runs. At the same time, it constitutes a limitation of the study. The model does not yet include the full physics of heat exchange in a refrigerated container, actual response delays of the refrigeration unit, variability in cargo load, or data transmission disturbances typical of IoT infrastructure under operational conditions. Further work should include validation of the model using data from real temperature monitoring systems. It would be particularly important to extend the experiments to include transmission delays, discontinuities in measurement signals, sensor errors, and variable sensor density within the cargo space. It would also be justified to compare EHO with other control and optimization algorithms, including threshold-based approaches and selected population-based metaheuristics. This would make it possible to determine whether the observed distributed control pattern results from the specific properties of the algorithm or from the structure of the multi-zone regulation model itself. The proposed concept provides a basis for further research on autonomous temperature control systems in the cold chain. The main conclusion from the simulations concerns not only the ability to maintain temperature within the admissible range, but also the way in which the system achieves this result. EHO does not enforce uniform behaviour across the entire container. Instead, it creates a distributed system of local responses. This property may be particularly relevant in maritime transport of pharmaceutical products, where thermal conditions change over time and quality risk often emerges locally before it becomes visible at the level of the entire cargo unit.

The proposed model provides a simulation-based proof-of-concept for adaptive multi-zone temperature control in an IoT-supported pharmaceutical cold-chain environment. The results show that the EHO-based controller can generate spatially differentiated cooling decisions and that temperature stabilization does not require permanent activation of the highest cooling mode in all zones. The combined analysis of temperature trajectories, control maps, switching counts, and cooling-mode shares indicates that regulation is local and asynchronous rather than globally synchronized. This property is relevant for maritime pharmaceutical transport, where thermal disturbances may occur locally because of insulation differences, solar exposure, door-side effects, and heterogeneous cargo-space conditions.

Author Contributions: Conceptualization, O.S., H.Z. and M.W.B.; Methodology, O.S. and H.Z.; Software, H.Z.; Validation, H.Z., M.D. and P.K.; Formal analysis, O.S., M.W.B., M.D. and P.K.; Investigation, O.S., H.Z., M.D. and P.K.; Resources, H.Z., M.D. and P.K.; Data curation, H.Z. and P.K.; Writing—original draft, O.S., M.W.B. and M.D.; Writing—review & editing, O.S. and H.Z.; Visualization, H.Z.; Supervision, O.S., H.Z. and M.W.B.; Funding acquisition, M.W.B. All authors have read and agreed to the published version of the manuscript.

Funding: This research received no external funding.

Data Availability Statement: All data generated or analyzed during this study are included in this published article.

Conflicts of Interest: The authors declare no conflict of interest.

References

1. Tsang, Y.P.; Choy, K.L.; Wu, C.H.; Ho, G.T.; Lam, C.H.; Koo, P.S. An Internet of Things (IoT)-based risk monitoring system for managing cold supply chain risks. *Ind. Manag. Data Syst.* **2018**, *118*, 1432–1462. [CrossRef]
2. Cil, A.Y.; Abdurahman, D.; Cil, I. Internet of Things Enabled Real-Time Cold Chain Monitoring in a Container Port. *J. Shipp. Trade* **2022**, *7*, 9. [CrossRef]

3. Apiecionek, Ł.; Biedziak, M. Fuzzy Adaptive Data Packets Control Algorithm for IoT System Protection. *J. Univers. Comput. Sci.* **2020**, *26*, 1435–1454. [CrossRef]
4. Zarzycki, H.; Ewald, D.; Prokopowicz, P. Leveraging Swarm Intelligence for Optimal Thermal Camera and Sensor Placement in Industrial Environments. *Electronics* **2024**, *13*, 601. [CrossRef]
5. Yang, Y.; Zhong, M.; Yao, H.; Yu, F.; Fu, X.; Postolache, O. Internet of Things for Smart Ports: Technologies and Challenges. *IEEE Instrum. Meas. Mag.* **2018**, *21*, 34–43. [CrossRef]
6. Yu, H.; Cui, X.; Bai, X.; Chen, C.; Xu, L. Incorporating graph theory and time series analysis for fine-grained traffic flow prediction in port areas. *Ocean Eng.* **2025**, *335*, 121693. [CrossRef]
7. Yu, H.; Wu, W.; Zhang, X.; Fang, Z.; Fu, X.; Xu, L.; Liu, J. Optimization-based global liquefied natural gas shipping network management for emission reduction. *Ocean Eng.* **2025**, *321*, 120366. [CrossRef]
8. Slowik, A. (Ed.) *Swarm Intelligence Algorithms (Two Volume Set)*; CRC Press: Cleveland, OH, USA, 2021.
9. Zarzycki, H.; Skubisz, O. A new artificial bee colony algorithm approach for the vehicle routing problem. In *Intelligent and Fuzzy Techniques for Emerging Conditions and Digital Transformation, Proceedings of the INFUS 2021 Conference, Istanbul, Turkey, 24–26 August 2021*; Springer International Publishing: Cham, Switzerland, 2022; Volume 1, pp. 562–569.
10. Zarzycki, H.; Ewald, D.; Skubisz, O.; Kardasz, P. A comparative study of two nature-inspired algorithms for routing optimization. In *International Workshop on Intuitionistic Fuzzy Sets and Generalized Nets*; Springer International Publishing: Cham, Switzerland, 2020; pp. 215–228.
11. Zarzycki, H.; Skubisz, O. An application of ant algorithm for routing optimization problem. In *International Business Information Management Association*; IBIMA Publishing: King of Prussia, PA, USA, 2021.
12. Skubisz, O.; Zarzycki, H. An Application of Particle Swarm Optimization Algorithm in the Sensor Placement Optimization Problem. In *Uncertainty and Imprecision in Decision Making and Decision Support—New Advances, Challenges, and Perspectives*; Springer: Cham, Switzerland, 2025.
13. Thrun, M.C.; Ultsch, A. Swarm intelligence for self-organized clustering. *Artif. Intell.* **2021**, *290*, 103237. [CrossRef]
14. Chen, X.; Cheng, F.; Liu, C.; Cheng, L.; Mao, Y. An improved Wolf pack algorithm for optimization problems: Design and evaluation. *PLoS ONE* **2021**, *16*, e0254239. [CrossRef] [PubMed]
15. Alyasseri, Z.A.A.; Khader, A.T.; Al-Betar, M.A.; Awadallah, M.A.; Yang, X.S. Variants of the flower pollination algorithm: A review. In *Nature-Inspired Algorithms and Applied Optimization*; Springer: Cham, Switzerland, 2018; pp. 91–118.
16. Yang, X.S.; Deb, S.; Zhao, Y.X.; Fong, S.; He, X. Swarm intelligence: Past, present and future. *Soft Comput.* **2018**, *22*, 5923–5933.
17. Yang, X.S. Swarm intelligence based algorithms: A critical analysis. *Evol. Intell.* **2014**, *7*, 17–28.
18. Xu, Y.; Li, Q.; Xu, X.; Yang, J.; Chen, Y. Research Progress of Nature-Inspired Metaheuristic Algorithms in Mobile Robot Path Planning. *Electronics* **2023**, *12*, 3263. [CrossRef]
19. Rahul, K.; Banyal, R.K. Metaheuristics Approach to Improve Data Analysis Process for the Healthcare Sector. *Procedia Comput. Sci.* **2022**, *215*, 98–103. [CrossRef]
20. Saini, M.; Maan, V.S.; Kumar, A.; Saini, D.K. Metaheuristic Algorithms and Their Applications in Performance Optimization of Cyber-Physical Systems Having Applications in Logistics. *Int. J. Syst. Assur. Eng. Manag.* **2024**, *15*, 2202–2217. [CrossRef]
21. Wang, G.G.; Deb, S.; Coelho, L.D.S. Elephant herding optimization. In *Proceedings of the 3rd International Symposium on Computational and Business Intelligence (ISCBI), Bali, Indonesia, 4–6 December 2015*; IEEE: Piscataway, NJ, USA, 2015; pp. 1–5.
22. Fong, S.; Deb, S.; Chaudhary, A. A review of metaheuristics in robotics. *Comput. Electr. Eng.* **2015**, *43*, 278–291. [CrossRef]
23. Wahid, L.Y.; Yab, N.; Hamid, R.A. A Meta-Analysis Survey on the Usage of Meta-Heuristic Algorithms for Feature Selection on High-Dimensional Datasets. *IEEE Access* **2022**, *10*, 122832–122856. [CrossRef]
24. Jarboui, B.; Siarry, P.; Teghem, J. (Eds.) *Metaheuristics for Production Scheduling*; John Wiley & Sons: New York, NY, USA, 2013.
25. Griffis, S.E.; Bell, J.E.; Closs, D.J. Metaheuristics in logistics and supply chain management. *J. Bus. Logist.* **2012**, *33*, 90–106. [CrossRef]
26. Hussain, K.; Salleh, M.N.M.; Cheng, S.; Shi, Y. On the exploration and exploitation in popular swarm-based metaheuristic algorithms. *Neural Comput. Appl.* **2019**, *31*, 7665–7683.
27. Euchi, J.; Yassine, A.; Chabchoub, H. The dynamic vehicle routing problem: Solution with hybrid metaheuristic approach. *Swarm Evol. Comput.* **2015**, *21*, 41–53. [CrossRef]
28. Ullrich, C.A. Supply chain scheduling: Makespan reduction potential. *Int. J. Logist. Res. Appl.* **2012**, *15*, 323–336. [CrossRef]
29. Nikolaev, A.G.; Jacobson, S.H. Simulated annealing. In *Handbook of Metaheuristics*; Springer: Boston, MA, USA, 2010; pp. 1–39.
30. Kalra, M.; Singh, S. A review of metaheuristic scheduling techniques in cloud computing. *Egypt. Inform. J.* **2015**, *16*, 275–295. [CrossRef]
31. Mor, B.; Shabtay, D.; Yedidsion, L. Heuristic algorithms for solving a set of NP-hard single-machine scheduling problems with resource-dependent processing times. *Comput. Ind. Eng.* **2021**, *153*, 107024. [CrossRef]
32. Fu, Y.; Hou, Y.; Wang, Z.; Wu, X.; Gao, K.; Wang, L. Distributed scheduling problems in intelligent manufacturing systems. *Tsinghua Sci. Technol.* **2021**, *26*, 625–645. [CrossRef]

33. Valouxis, C.; Gogos, C.; Alefragis, P.; Goulas, G.; Voros, N.; Housos, E.D. DAG Scheduling using Integer Programming in heterogeneous parallel execution environments. In Proceedings of the Multidisciplinary International Scheduling Conference, MISTA, Ghent, Belgium, 27–30 August 2013.
34. Ramezani, F.; Lu, J.; Taheri, J.; Hussain, F.K. Evolutionary algorithm-based multi-objective task scheduling optimization model in cloud environments. *World Wide Web* **2015**, *18*, 1737–1757. [CrossRef]

Disclaimer/Publisher's Note: The statements, opinions and data contained in all publications are solely those of the individual author(s) and contributor(s) and not of MDPI and/or the editor(s). MDPI and/or the editor(s) disclaim responsibility for any injury to people or property resulting from any ideas, methods, instructions or products referred to in the content.